Instrument Science Report ACS 2012-05

A new accurate CTE photometric correction formula for ACS/WFC

M. Chiaberge
October 03, 2012

ABSTRACT

We present a new CTE photometric correction formula based on observation of 47Tuc obtained during Cycles 17, 18 and 19. Images were taken with two filters and different exposure times, in order to sample a wide range of background levels. In addition, the Cycle 19 program included imaging of a denser field near the center of 47Tuc with the F502N filter. Thanks to the increased number of stars available for the analysis, we are able to characterize CTE losses down to the lowest background levels (down to ~0.2e$^-$) without significant loss of accuracy with respect to higher sky levels. The data from these three Cycles allow us to derive a new form of the correction formula that is significantly more accurate that those previously published. The formula may be used to correct stellar photometry for CTE losses on drizzled images taken after SM4. We compare the results of our new CTE correction to previous versions of the correction formula for ACS/WFC, and with the pixel-based CTE correction that is currently available as part of CALACS. The formula presented in this ISR and the pixel-based correction are in substantial agreement at high stellar fluxes and for relatively high background levels. However, the former is significantly more accurate than the latter for faint stars superimposed to a low sky background.

Introduction

CCDs in space are exposed to radiation damage which may strongly decrease the Charge Transfer Efficiency (CTE). This is explained in terms of an increase of the imperfections in the crystalline lattice of the CCD due to the bombardment of energetic charged particles in the space environment (Pickel et al. 2003, Srour et al. 2003, for reviews). This

generates an increasing number of charge traps which lower the charge transfer efficiency of each pixel of the detector. CTE is defined as (1-CTI), where CTI = ΔQ/Q is the fractional charge lost during each single transfer (Charge Transfer Inefficiency). A perfect CCD would have CTE=1 (CTI=0).

Since 2003, specific calibration programs aimed at characterizing the effects of the CTE on stellar photometry were performed (Riess, ISR ACS 2003-009). First characterizations of the effects of a decreasing CTE for WFC were made by Riess & Mack (ISR ACS 2004-006). Meanwhile, results from the internal CTE calibration programs showed that CTE appears to decline linearly with time, and that CTE losses are stronger for lower signal levels (Mutchler & Sirianni ISR 2005-03). However, in order to derive an accurate correction formula for photometry, a number of observations at different epochs and for different levels of sky background and stellar fluxes have to be accumulated. In Chiaberge et al. ISR 2009-01, we showed the results of the observations taken through March 2006, which, coupled with a different approach in the data analysis, allowed us to significantly improve the CTE photometric correction formula. However, following the failure of the Side 1 of the Low Voltage Power Supply and the switch to Side 2, the temperature of the WFC was lowered from -77 to -81C. Such a temperature change affected the overall performance of the detector, and in particular its sensitivity, the rate/number of hot pixels, and also the properties of the CTE (see e.g. Mack et al. ISR 2007-02, Ubeda & Anderson ISR 2012-03).

Recently, a pixel-based CTE correction became available for ACS/WFC (Anderson & Bedin ISR 2010-03), and it was included in the OTFR data processing pipeline in the spring of 2012. However, a photometric correction formula is still needed, both for the ACS Team to continue monitoring the CTE variations, and for users that may prefer to perform photometry on uncorrected images. This option is recommended in particular for regions of the parameter space where the pixel-CTE correction is less reliable (e.g. for the lowest flux levels and for low sky background values). A further advantage is that while the pixel-based correction produces images in which the noise level is higher than in the original data, in general that is not the case for photometry corrected using the CTE formula.

In this ISR we present the results of the analysis of the post-SM4 External CTE monitor calibration programs. With respect to previous programs, we made further improvements both to the observing strategy and to the statistical analysis of the results. This led us to achieve two important results: i) we found a different dependence of the CTE on stellar flux and sky background, as compared to the previous formula; ii) we derived a correction with a significantly higher level of accuracy.

Data

The observations were taken as part of calibration programs CAL/ACS 11880, 12385, 12730 (PI: M. Chiaberge). The target of the observing program is a field ~7' West off the core of the globular cluster 47 Tucanae. We image the field with WFC at the initial position, and then we utilize 2 large slews (102"), i.e. half the size of the WFC. The slews

are performed both in the X and in the Y directions in the detector framework, to vary the number of transfers for each star in the field and to check both serial and parallel CTE, respectively. For reference, in Fig. 1 we reprint a figure from Riess (ISR ACS 2003-009) which illustrates the observing strategy. For example, a star located at Y=100 in the FLT file framework when observed with WFC2 (image at position "0,0"), will also fall at Y=100 when observed on WFC1 after the slew is performed (image position "0,1"). However, the star undergoes Y-transfers$_{WFC2}$=100 and Y-transfers $_{WFC1}$=2049-100 when it is read out from WFC2 and WFC1, respectively. Such a pair of images is used to check parallel CTE, by comparing the measured magnitudes of stars in the two images. For serial CTE, the shift is performed in the X direction, and the images "0,0" and "1,0" are used.

Images are taken using two different filters (F502N and F606W) and with a range of exposure times (between 30s and 400s), in order to sample at least five different background levels.

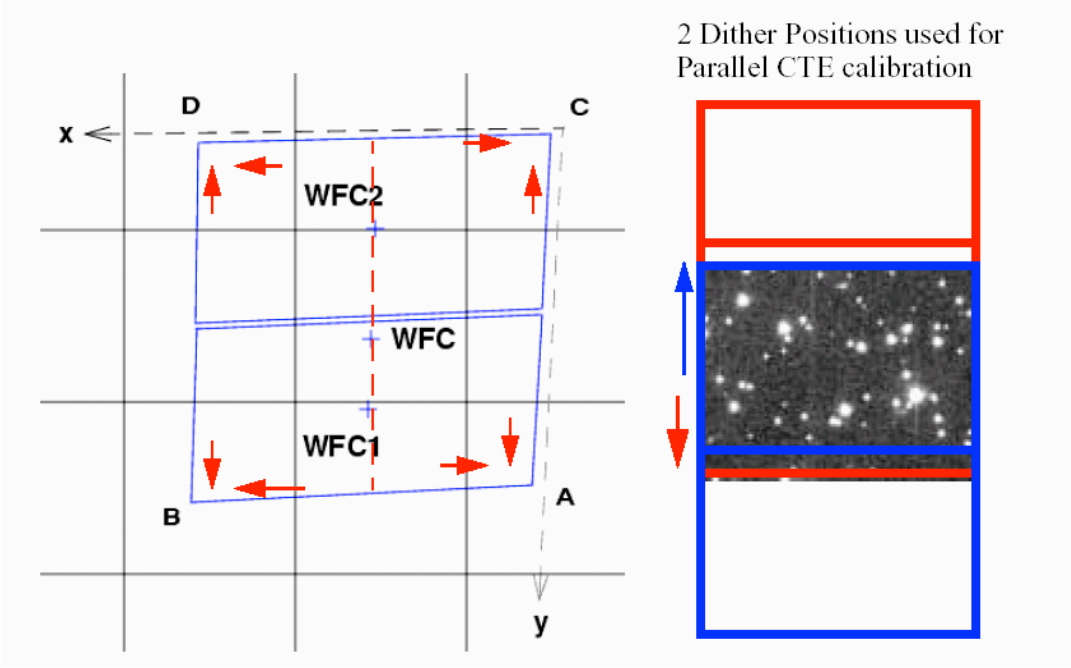

Figure 1: The location of the 4 WFC amplifiers and the readout direction are reported in the left panel of the figure. In the right panel, we show a schematic of the 2 dither positions used to check parallel CTE (figure taken from Riess ISR ACS 2003-009).

Two CR-SPLIT images are taken for each pointing, in order to facilitate cosmic ray rejection.

In Cycle 19 we also imaged a region closer to the center of 47Tuc, about 3' SW off the cluster core. For that field we used the F502N filter and 30s exposure time. The aim of this observation is to provide a larger number of stars on a low sky background level (~0.5 e^-). In fact the statistics provided by the standard field is not sufficient to constrain the parameters of the CTE correction formula down to the lowest sky levels.

In the following we outline our analysis procedure and we present the improved time dependent formula to correct aperture photometry for point sources.

Data Analysis

The data are retrieved from the MAST archive and are processed through the standard OTFR pipeline, to produce calibrated *FLT* files. For each observation epoch, and for each filter/exposure time configuration, two WFC images at each of the three positions (0,0), (1,0) and (0,1) were taken. The images are aligned to match the same coordinate system using the *tweakshifts* task available in *Pyraf*. To that aim, we use a script that iteratively uses that task to achieve an image registration accuracy higher than 0.1 pixels. When the residual offsets between images converge to the desired value, *multidrizzle* is used to produce a "master" image (corrected for geometric distortion) for each filter/exposure time combination composed of all of the six images taken with that configuration (2 CRSPLITs x 3 positions). *Multidrizzle* identifies image defects such as hot pixels, saturated pixels, and pixels that were hit by cosmic rays, and populates the "data quality" extension of each of the *FLT* files with the appropriate code to identify the nature of each of the affected pixels. We use the same task to produce cosmic ray-rejected images for each of the three positions (0,0), (0,1) and (1,0). Cosmic rays are also iteratively removed as part of *multidrizzle*. We then mask out regions of 50 pixel radius around each of the saturated stars. Stars affected by hot pixels are not removed, but since hot pixels are evenly distributed across the chip, such artifacts do not significantly affect our CTE measurements.

We perform aperture photometry on a star list obtained by running the task *daofind* in the IRAF package *daophot* on the "master" image. Stars from the complete list are then re-centered on each of the single_sci images, and photometry is performed using the task *phot,* after rejection of all stars that lie within the masked out areas. All stars that have S/N = 3 or higher on each image are included in the analysis. The photometry aperture radius is set to 3 pixels. This ensures that reliable aperture photometry can be performed on both faint and bright stars. The background is measured locally, in an annulus of inner radius r=13 pixels and d=3 pixels wide.

In the following, we focus mainly on parallel CTE (i.e. CTE in the y-direction). However, we checked that the CTE effect in the x-direction (serial CTE) is still unmeasurable in our data.

Results

Magnitude losses for different bins of stellar flux and sky background

For each epoch, filter and exposure time combination, stars are grouped in bins of stellar flux (in e^-) measured in each "pair" of images (0,0 and 0,1). Each star is assigned to a particular flux bin based on the lowest flux measured in each "pair". In most cases six bins are obtained. Note that at this stage no aperture correction is performed. Bright stars in the field used for the observations increase the background level over large regions

across the images. Since the CTE depends strongly on the background level, we restrict the analysis to stars in a narrow range of background levels. For a few configurations, we have enough stars in the field to allow more than one bin of sky levels, e.g. including stars superimposed to regions located in the halos of the brightest stars in the field of view.

For each bin of flux level and sky background, the magnitude difference between stellar fluxes measured in each pair of images (positions "0,0" and "0,1") $\Delta mag = m_0 - m_1$ is plotted against the number of Y-transfers each star undergoes during read out. This is calculated by transforming the coordinates of each star on the chip back from the DRZ to the FLT framework. More precisely, ΔY-transfers = Y-transfers$_0$ -Y-transfers$_1$, i.e. the difference between the number of transfers in the two images, is used. Negative and positive values of ΔY transfers correspond to stars positioned on different sides of the chip. For example, a star located at Y=2048 on WFC2 will be located approximately at Y = 1 in the image taken with WFC1, and in this case ΔY transfers = 2047. A star located at Y=2048 on WFC1 will be located approximately at Y = 1 in the image taken with WFC2, and in this case ΔY transfers = -2047. In other words, stars that are located far from the amplifiers (i.e. near the chip gap) have $|\Delta Y| \sim 2000$. $\Delta mag_{|\Delta Y|=2000}$ is thus the actual magnitude loss for stars on the opposite side of the chip with respect to the amplifiers.

A non-weighted linear fit to the data is performed, and outliers are rejected using iterative sigma-clipping. After four iterations, the value of Δmag_{2000} i.e. the value of Δmag for 2000 pixel transfers is derived from the slope of the linear regression. This approach assumes that 1) the two WFC chips have the same CTE properties; and 2) the CTE losses are a linear function of the number of transfers. Assumption 1) is supported by the fact that the ACS WFC chips were obtained from the same CCD wafer. Assumption 2) is a reasonable assumption based on the homogeneity of the detector's physical characteristics. Both assumptions are also clearly supported by the results shown below in Fig. 1 and 2, in which neither significant deviations from a linear dependence, nor significant offset in Δmag at Y=0 are observed.

In Fig. 1 we show results from observations taken in November 2011 with the F606W filter. The red line in each box is the linear fit, while the yellow lines indicate the rms uncertainty on the slope. Because of the better statistics achieved in the latest cycles as compared to previous observations (see Chiaberge et al. ACS ISR 09-01), the results of the fit are accurate enough that the yellow lines almost overlap with the red line in most cases.

It is interesting to show the results for the lowest sky background (< 1e$^-$), which is obtained using the F502N filter and 30s exposure time. In Fig. 2 (top panel) we show the results obtained using the standard 47Tuc field 5' off the center. In the bottom panel of the same figure we show the same plots obtained using stars in the new field we observed during Cycle 19, which is closer to the core of the cluster and returns a much larger number of stars. It is clear that the new field allows us a significantly higher accuracy.

The fits allow us to robustly estimate the CTE losses at the edge of the chip, on the opposite side of the amplifiers. For each bin of stellar flux, we calculate the CTE loss for 2000 transfers, and its rms uncertainty.

The next step is to model the dependence of the magnitude losses at Δy=2000 on the stellar flux, and see how that also depends on the sky background. The final step is then to find the best representation of the time dependence. In Chiaberge et al. ACS ISR 2009-01 and in previous work (e.g. Reiss & Mack 2004-06) the assumed form of the CTE correction formula was

$$\Delta mag_{loss} = 10^{a} \times SKY^{b} \times FLUX^{c} \times (Y_{tran}/2000), \quad (1)$$

where a, b, and c are free parameters determined from fitting the data, and Y_{tran} is the number of transfers. Such a formula implies that the losses have a linear dependence in log(Δmag) v log (FLUX) and in log(Δmag) v log (SKY) plots. However, while such an approximation is sufficient when the CTE losses are relatively small (i.e. in pre-SM4 HST Cycles), post SM4 data show significant deviations.

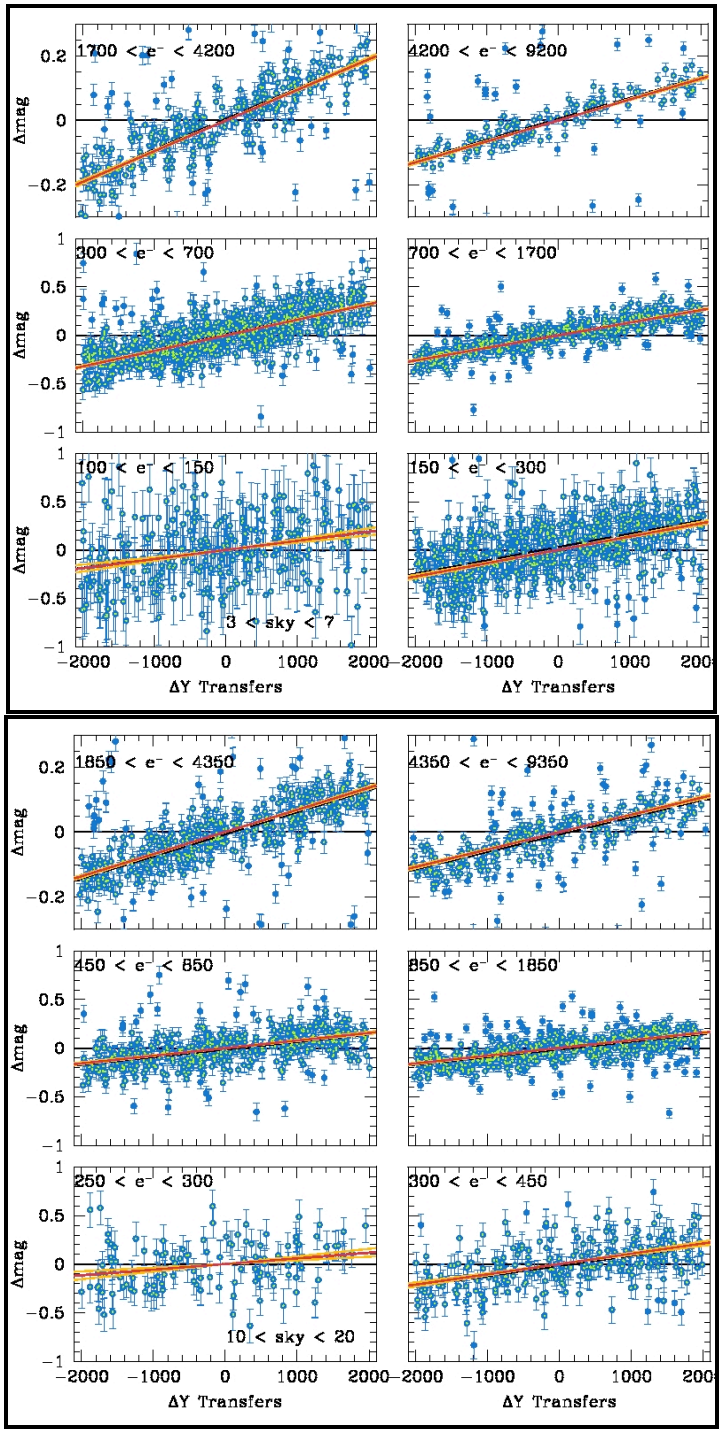

Figure 1: Results for different bins of stellar flux and different levels of sky background. Δmag is the difference between the magnitudes measured in images taken at position "0" and "1". ΔY-transfers is the difference in number of transfers for each star between image "0" and image "1" (see text). Data are from November 2011, F606W, exp. time is 40s (top panel) and 150s (bottom panel). Filled blue circles are rejected outliers. The black dashed lines (where visible) are linear fits to the data, and the red line is the same fit shifted so that the value of the intercept is 0. The yellow lines correspond to 1-σ error on the slope of the fit. The considered bin of stellar flux is reported in each box.

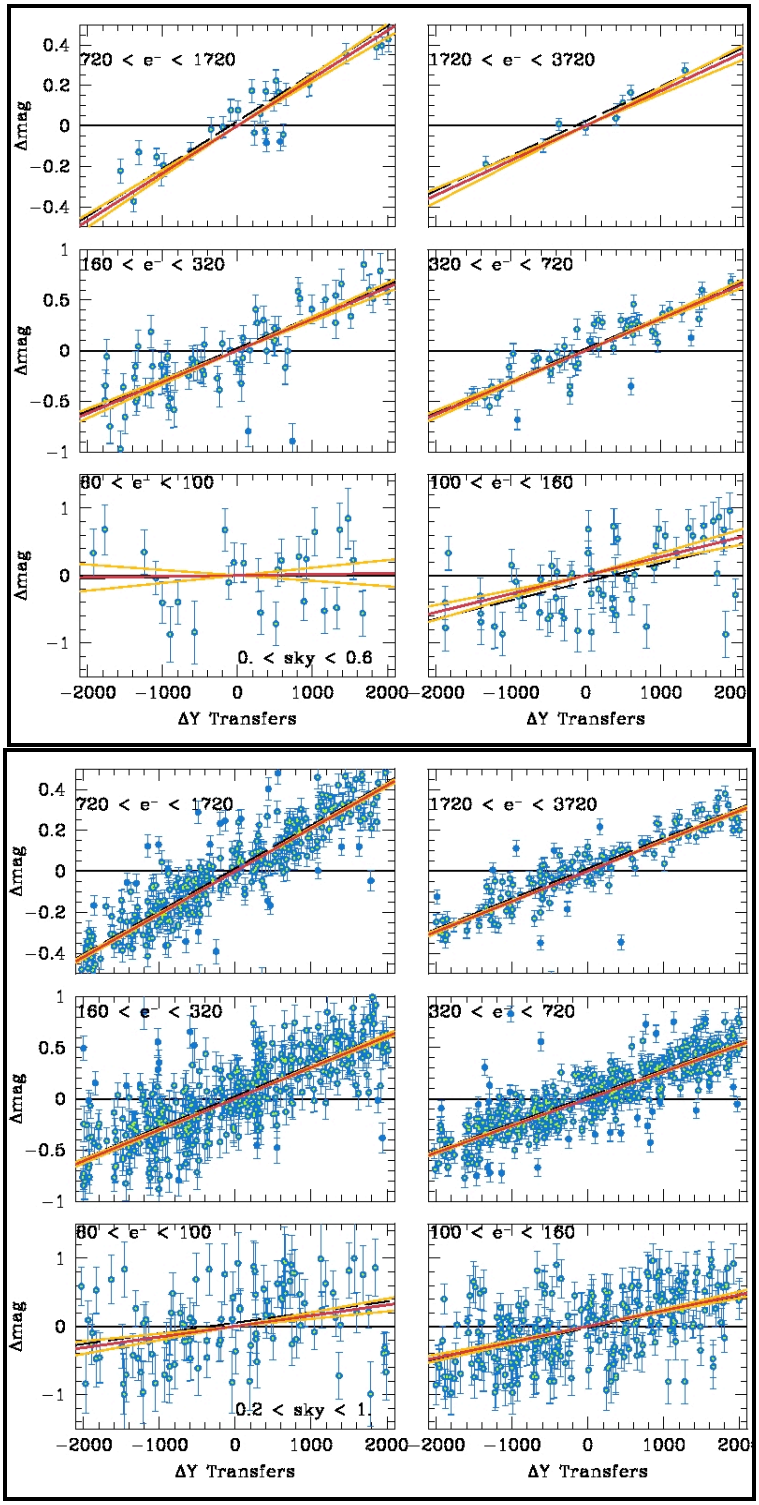

Figure 2: Results for the lowest sky backgrounds, obtained using the F502N filter and 30s exposure time. The top panel shows stars from the standard 47Tuc field 5' off the core, while the bottom panel shows the results of the observations taken on the new target, which is a denser filed closer to the cluster center. Note that the sky level in the bottom panel is slightly higher than the one in the top panel. This is because the field 3' off the cluster core is more crowded than the standard calibration field.

In Fig. 3 (left panel) we show data taken with a sky level of ~0.6 e^-, again using the field close to the cluster center, the F502N filter and 30s exposure time. It is quite clear that the deviations from a simple linear dependence in a logarithmic space are significant, both at the lower and higher ends of the stellar flux distribution. At low fluxes, the apparent "increase" of the CTE is only due to incompleteness. The CTE losses are so large that a significant fraction of low flux stars are below the detection threshold in the image in which they are located far from the amplifiers. This is demonstrated by performing the photometry using a higher S/N threshold. We observed that the turnover shown in Fig. 3 (left) shifts towards higher fluxes (i.e. the sample becomes incomplete at higher fluxes for increasing S/N thresholds). In Fig. 3 (right panel) we show the effect of setting the threshold at S/N = 5 (blue points) and 10 (yellow points). Therefore, for each sky background level, we identify the flux level at which our sample of stars becomes to suffer from incompleteness, and we eliminate the points that lie at fluxes lower than the turnover.

Such a turnover might be erroneously interpreted as an improvement of the CTE at low fluxes (e.g. as a result of the 3μ mini-channel implant originally performed on the ACS detectors). However, the fact that it is present at all background levels, and that the "peak" is located at an almost constant value of the S/N are further hints that it is not due to the characteristics of the instrument. We recommend users to be extremely careful when using correction formulae to correct the photometry at low S/N, because incompleteness effects may severely impact the measurements.

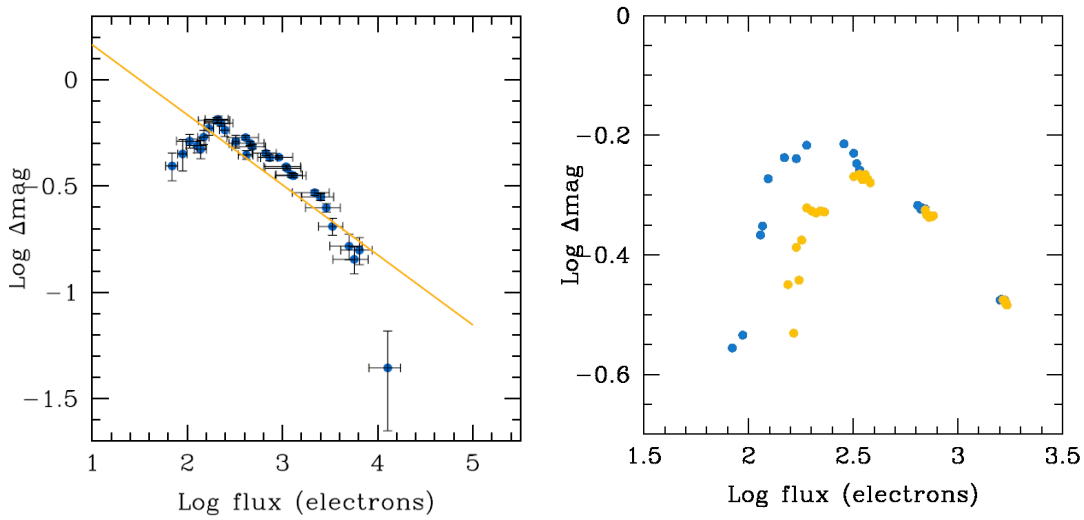

Figure 3 Left: Magnitude loss at Δy=2000 as a function of the stellar flux. The yellow line is a linear fit to the data and it is plotted just to better show the deviation from a simple linear dependence in a logarithmic space. The errorbar in the X axis represents the width of each bin of stellar flux. The large number of bins is simply obtained by re-binning the data with various combinations of flux center and width. **Right:** The effect of setting the S/N at different levels (blue = 5, yellow = 10) proves that the turnover observed at low fluxes is due to incompleteness (see text for more details). We do not plot errorbars for clarity.

In Fig. 4 we show that once the "clean" datasets are considered, there is a tight linear dependence between the magnitude loss at Δy=2000 and the log of the flux in electrons. In the figure, we show data for two different sky background levels (~0.6 and ~14 e^-). This analysis is performed for the Cycle 19 data, where the improved statistics at the lowest background levels allow us significantly higher accuracy. The models are then tested against the data taken in the previous cycles (17 and 18).

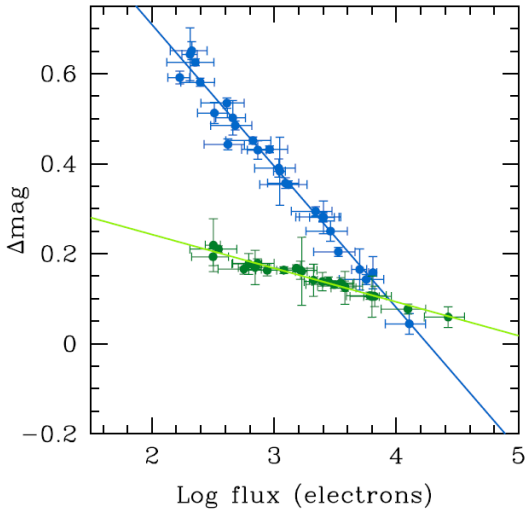

Figure 4: Magnitude loss after 2000 transfers plotted vs the Log of the stellar flux in electrons. Blue and green points are for sky background levels of ~0.6 and ~14 e^-, respectively. The solid lines are weighted linear fits to the data.

Therefore, we conclude that the correct linear dependence is of the kind

$$\Delta mag_{\Delta y=2000} = \alpha \, Log(FLUX) + \beta,$$

where both the α and β coefficients depend on the sky background level. In Fig. 5 we show that a simple linear model is also able to represent the dependence of both those coefficients on the sky level. Therefore, we can write both α and β as

$$\alpha = p \, Log\,(SKY) + q\,, \quad \beta = p' \, Log(SKY) + q'$$

where the coefficients p, p', q, q' are derived from the linear fit.

Summarizing, the magnitude losses can be modeled using the following formula:

$$\Delta mag(Y) = [p \, Log(SKY) \, Log(FLUX) + q \, Log(FLUX) + p' \, Log(SKY) + q'] * Y_{tran}/2000, \qquad (2)$$

where Y_{tran} is the number of transfers. Note that the coefficients p, q, p' and q' carry the information on the time-dependence of the CTE losses, since they are different at each epoch.

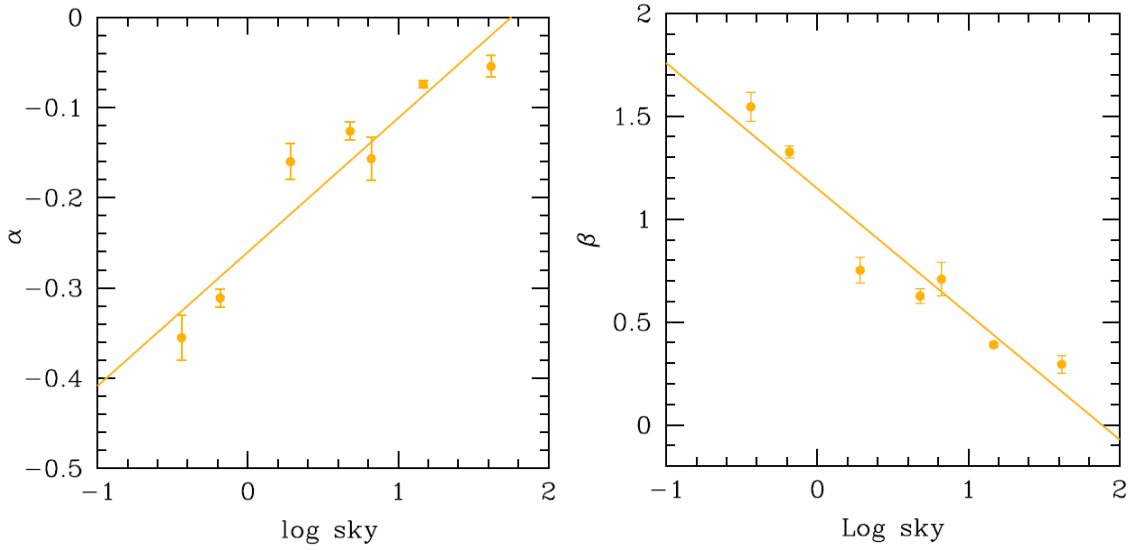

Figure 5: Coefficients α, β as a function of the sky background level. The solid lines are weighted linear fits. Reduced χ^2 are 1.18 and 1.16 for the left and right panel, respectively.

Statistical analysis

In order to derive the coefficients with the highest possible accuracy, we use the package "R" and different fitting routines. In Table 1 we report the results of linear fits for Cycle 17, 18 and 19.

We performed fits for the three epochs separately, using the following model

y = a*AB + b*A + c*B + d

where in our case $y=\Delta mag_{\Delta Y=2000,}$ A = log(FLUX), B= log(SKY) and a, b, c and d are the coefficients p, q, p' and q', respectively. All data ($\Delta mag_{Y=2000}$, SKY, FLUX) are simultaneously fitted. We use the *lm* and *rlm* regression routines and different values for the weights. The *rlm* routine (which is part of the "MASS" package) performs robust regression using different weight methods and M-estimators. The fits are performed using an iterated re-weighted least squares method. The *lm* routine is a less sophisticated routine which is also based on least squares fitting (see e.g. Chambers 1992, Huber 1981).

Depending on the used dataset, either of these methods can provide good results. We perform a careful statistical analysis of the results obtained with all of the above methods using "R", and we find that in most cases the results of the weighted and non weighted methods are statistically indistinguishable. However, for the data taken in Cycle 18 the results obtained using *lm* and a non-weighted linear fit have significantly smaller residuals and the residuals show smaller trends with fitted values (see Fig. 5). While this

may happen if the weights are not optimally chosen, large trends imply significant deviations from a normal distribution of the residuals. Therefore, we use the coefficients obtained with *lm* as our best fit values.

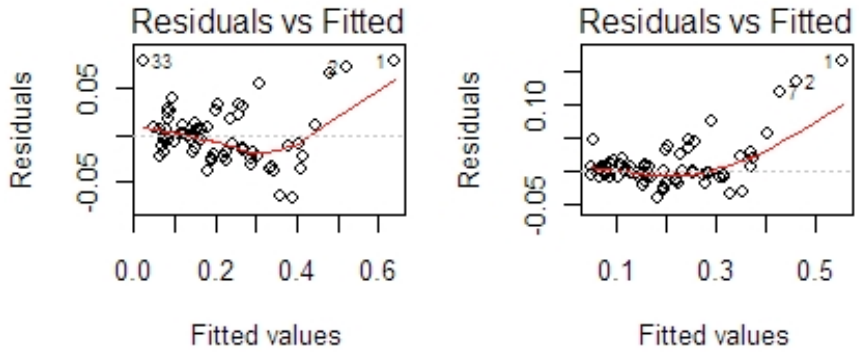

Figure 6: Residuals v fitted values for two different fitting routines. Left: *lm* non weighted; Right: *rlm* weighted, M-estimator with a Huber Psi function. The residuals are significantly smaller, and smaller trends are observed in the left panel.

In Table 1 we report the results of the fits for all of the coefficients and for the three epochs. In the table we also report the results of the t-statistics for each parameter and the residual standard error of the fit for each epoch. It is worth noting that the probability that t is larger than the calculated value P(>|t|) is $< 2 \times 10^{-16}$ for all of the parameters.

For comparison, we also report in Table 2 the results of the statistical analysis performed assuming model (1), i.e. the formula used in e.g. Riess & Mack ACS/ISR 2004-06 and Chiaberge et al. ACS/ISR 2009-02. The values obtained for Cycle 19 only are reported, since the purpose is just to provide the reader with statistical evidence that the previously used model is less accurate than model (2).

Table 1. Linear fit results for the coefficients for Cycle 17, 18 and 19. Column (1): coefficient name for each cycle; (2): coefficient values; (3): standard error for each coefficient; (4): value of the t variable (larger positive and negative values indicate more accurate fitted values for the coefficient); (5) residual standard error of the fit, for each epoch.

Coefficient (1)	Value (2)	Std. error (3)	t-value (4)	Res. Std. error (5)
Cycle 17				0.02245
p	0.1133	0.0057	19.80	
q	-0.2033	0.0053	-37.68	
p'	-0.4736	0.0181	-26.19	
q'	0.9115	0.0166	54.80	
Cycle 18				0.02945
p	0.1324	0.0088	14.95	
q	-0.2201	0.0092	-23.91	
p'	-0.5516	0.0304	-18.13	
q'	0.9913	0.0296	33.48	
Cycle 19				0.03126
p	0.1764	0.0097	18.17	
q	-0.2681	0.0079	-33.87	
p'	-0.7032	0.0314	-22.41	
q'	1.1706	0.0244	47.95	

Table 2: Same as for Table 1, but for Cycle 19 only. The fitted parameters correspond to model (1) used in previous ISRs (see text).

Coefficient (1)	Value (2)	Std. error (3)	t-value (4)	Res. Std. error (5)
Cycle 19				0.0806
a	0.5243	0.0472	11.09	
b	-0.2186	0.0134	-16.32	
c	-0.3371	0.0150	-22.52	

Time dependence

In Fig. 7 (left panel) we show the values of the coefficients p, q, p' and q' plotted against time (in days from the ACS launch). The solid lines in the figure are weighted linear fits. Three epochs only are not sufficient to draw firm conclusions on the time dependence,

but it is reasonable to assume that the coefficients vary linearly with time. Note that differently from previous work, we do not assume that CTE=1 at $T=t_{launch}$. Although such an assumption is a reasonable approximation, it is not formally correct, since it is known that CTE was not perfect even in ground testing. Furthermore, following both the ACS temperature change and the ACS repair performed as part of SM4, we cannot assume that the CTE losses follow the same time-dependence as before. Evidence for a change in the time dependence is clearly shown by the behavior of CTE losses for hot pixels (Ubeda & Anderson ACS/ISR 12-03). This is also seen in our data: in fact, if we extrapolate the values of the coefficients back to e.g. March 2006, when observations from the last pre-SM4 External CTE monitor programs were performed, the results are significantly off (Fig. 7, right panel).

The results shown in Fig. 7 bring further support to the hypothesis that the CTE time dependence can be approximated with linear models. Therefore, we can rewrite the four coefficients p, q, p' and q' as p(t), q(t), p'(t) and q'(t), and each of them can be parameterized as $k(t)=k_1*t+k_2$ (where k is any of the above coefficients, and k_1 and k_2 are the slope and the intercept of each of the parameterizations). We can thus rewrite the CTE correction formula using such parameterizations, and we obtain the time-dependent CTE photometric correction formula:

$$\Delta mag\,(Y, t, SKY, FLUX) = \qquad (3)$$

$$[p_1\ Log(SKY)\ Log(FLUX)\ t\ +\ p_2\ Log(SKY)\ Log(FLUX)\ +\ p'_1\ Log(SKY)\ t\ + \\ +q_1 Log(Flux)\ t\ +\ p'_2\ Log(SKY)\ +\ q_2 Log(FLUX)\ +\ q'_1\ t + q'_2]\ *\ Y_{tran} / 2000,$$

where t is the time of the observation (in modified Julian days, e.g. August 24th 2012 at 0h 0m 0s = MJD 56163.5), FLUX is the flux (in e^-) measured within a 3-pixel aperture radius, SKY is the background level measured as close as possible to the star and Y_{tran} is the number of transfers.

In Table 3 we report the values of the linear fits for the time dependence of the coefficients. The parameters were obtained by performing a global fit using *lm* (see above), simultaneously using the results from all of the three post-SM4 epochs. It is clear that only three epochs are not sufficient to derive results that can be reliably extrapolated far outside the range considered in this ISR (i.e. between Cycle 17 and 19). However, as we show in the following, the formula produces accurate results if used for observations performed within such a time frame.

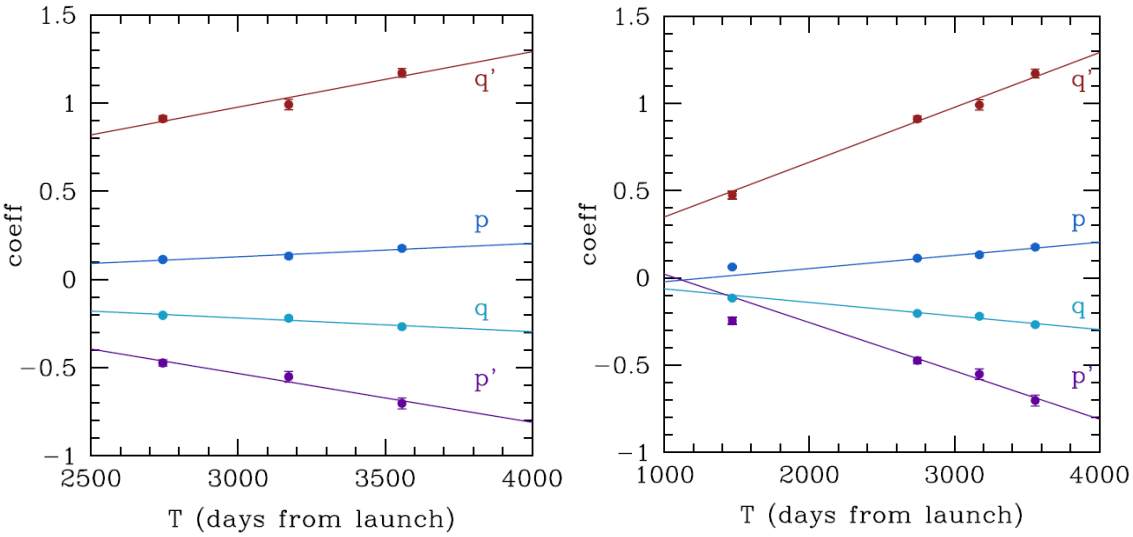

Figure 7: Left panel: coefficients of model (2) as a function of time from launch (in days). Right panel: same as for the left panel, but the value of the coefficients for March 2006 are also shown.

Table 3: Parameters of the time dependence of the model coefficients obtained by fitting all post-SM4 epochs together. The slope and the intercept of the linear fits are given, together with the errors on the fit. The residual standard error for the fit is 0.028 on 259 degrees of freedom, the p-value is $< 2.2 \times 10^{-16}$.

Coefficient	**Slope**	**σ**	**Intercept**	**σ**
(1)	**(2)**	**(3)**	**(4)**	**(5)**
p	$p_1 = 5.624 \times 10^{-5}$	1.219×10^{-5}	$p_2 = -2.985$	0.676
q	$q_1 = -7.345 \times 10^{-5}$	1.201×10^{-5}	$q_2 = 3.845$	0.666
p'	$p'_1 = -2.164 \times 10^{-4}$	3.954×10^{-5}	$p'_2 = 11.44$	2.194
q'	$q'_1 = 3.010 \times 10^{-4}$	3.712×10^{-5}	$q'_2 = -15.68$	2.059

In Fig. 8 we show the accuracy of the correction formula (3) as a function of sky background and stellar flux. The errors are calculated for observations taken on January 1st, 2011, but are valid throughout the whole period covered by Cycle 17, 18 and 19. The estimate of the error was obtained by calculating the predicted CTE loss (at ΔY=2000 transfers) for different regions of the parameter space, and calculating the error for 68% confidence level. The accuracy of the formula is better than 4% for all of the region of the parameter space considered in the figure. This has been chosen to sample the level of sky background and stellar flux typical of most of the ACS/WFC observations in which CTE may be an issue.

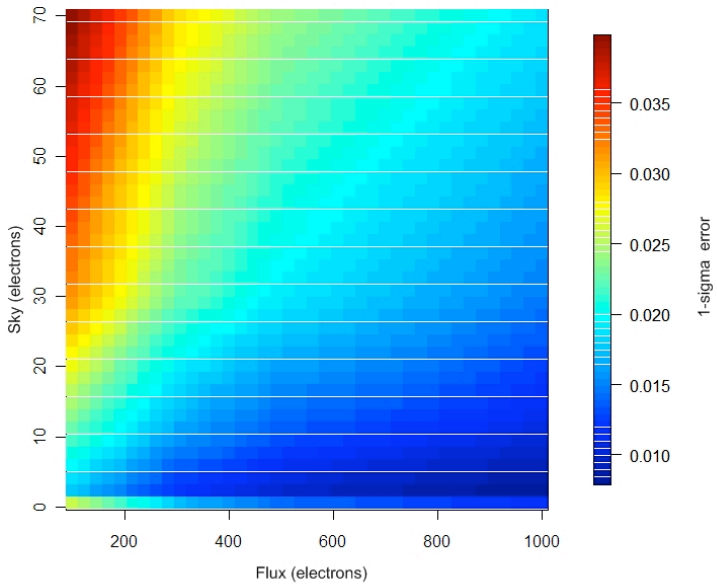

Figure 8: CTE formula error map. 1σ errors are plotted in a color scale as a function of sky background level and stellar flux.

CTE correction tests

We tested the CTE correction formula by applying it to the stellar photometry and by checking the residual magnitude loss. In Fig. 9 (left) we show the extreme case of the image taken with F502N and 30s exposure time (which has an average sky background level of ~0.6 e^-). In the top panel of that figure, we report the magnitude residuals vs the number of transfers each star undergoes ΔY Transfers. The number of transfers is the absolute value of that quantity. Therefore stars far from the amplifiers have |ΔY| ~ 2000. The residuals are calculated as in Figs. 1 and 2 as the difference between the magnitude

of the stars measured in each of the two pointings. The red line is the linear fit to the data, renormalized at Δmag = 0 for ΔY = 0. Note that in this case all of the stars in the field of view are plotted in the same figure (from flux=150e^- to flux = 200,000e^-). While the average losses at the edge of the chip, far from the amplifiers, are ~0.6 mag (top panel of the left plot), once the photometry is corrected using the formula derived above the average losses are <10% even in the extreme case in which the background is close to 0e^- (bottom). Fig. 9 (right) shows the same test performed on the image taken with the F606W filter and 150s exposure time, where the background is around 15 e^-. In this case, the residual average losses for stars with flux > 100 e^- at the edge of the chip, on the opposite side of the amplifiers, is extremely small. The top panel shows the uncorrected data, in which an average loss of 0.12 magnitude at the edge of the chip is measured. A slight overcorrection is observed in the lower panel, which shows the data after CTE correction, but the photometry is recovered to better than 1%, on average. Note that in both cases the spread does not increase once the CTE correction is performed.

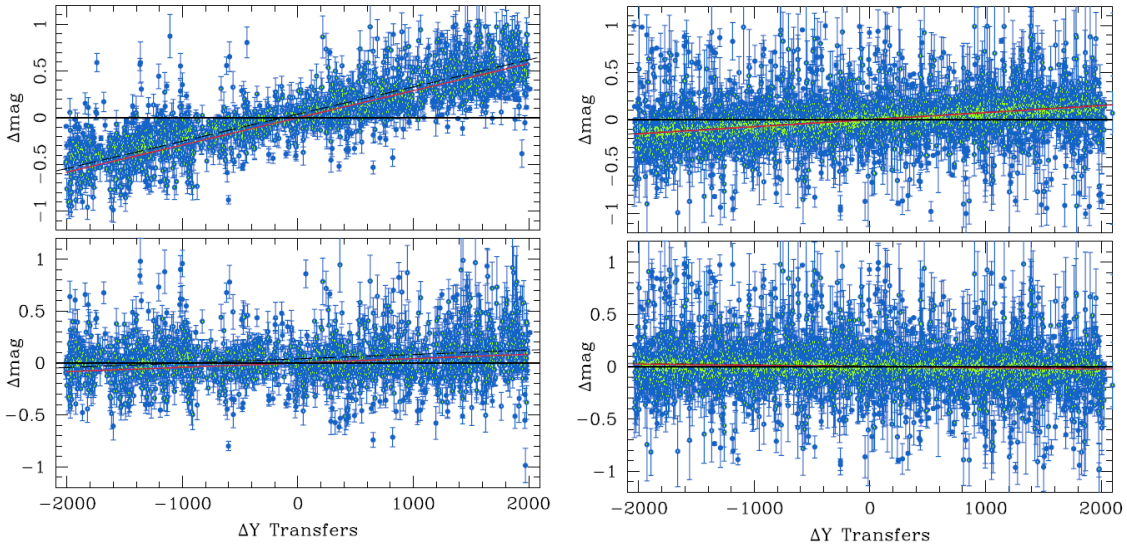

Figure 9: Test of the accuracy of the CTE correction. Left: photometry of all stars with flux>150e^- in the field 3' SW off the center of 47Tuc observed with F502N and 30s exposure time. The top panel shows the residuals from uncorrected photometry, while the bottom panel shows the same data after CTE correction. Right: Same as for the left figure, but for the data taken with F606W and 150s exposure time.

Validity of the CTE correction formula at low S/N levels: is there any evidence for improved CTE at low fluxes?

A further test we perform is aimed at ensuring that the assumption that the turnover seen at low fluxes in Fig. 3 is only due to incompleteness of the stellar catalog, and that there is no evidence for any improvement of the CTE at low stellar fluxes (and for low S/N ratio, irrespective of the stellar flux).

We firstly create a catalog of stars using the deep image taken with the F606W filter and 400s exposure time. We measure the flux of all of the detected stars in that image, and then we use the same catalog to find the same stars in the short exposure (30s) taken with the F5052N filter. Only a small fraction of the stars included in the catalog are "visible" in the short exposure, but using the positions on the chip derived from the deep exposure we can perform aperture photometry even if the stars are detected at a very low S/N level. Using bright stars in the F606W image (~300,000e^- or higher) we derive that the flux ratio between the two images is ~0.1%, having rejected a few outliers. Therefore, we expect to see that, after CTE correction, such a ratio of ~0.1% is observed for stars of all fluxes, while the spread is expected to significantly increase towards lower fluxes.

In Fig. 10 we show the results of such a test. The flux of each star in the F502N short exposure, as a percentage of the flux as measured in the deep exposure, is plotted against the Y coordinate of the star in the FLT frame (0 to 2048 for WFC2, 2049 to 4096 for WFC1). Stars are plotted in different panels according to their flux in the deep exposure. In the figure on the left hand side, we show the results before correction. The characteristic "V" shape appears as a result of the fact that CTE losses increase as the distance to the amplifiers increases. Note that the "V" shape is less clearly seen at lower fluxes, where the noise in the short exposure with F502N significantly affects the photometry accuracy. For fluxes <20,000e^- in F606W (i.e. <20e^- in F502N) the background noise in the short exposure largely dominates the distribution of the points in the plot. On the right hand side of the figure, we plot the same data after CTE correction. The red lines are linear fits that are only used to guide the eye in identifying the average flux. The red line is not plotted in the box with the faintest stars, because in that range of flux the results are just dominated by noise. The results clearly show that the 0.1% fraction seen in the box in which the brightest stars are plotted is also found for lower flux stars, albeit with an increasing scatter, with the only possible exception of the faintest stars, where the background noise in the short exposure dominates the measurements. The only caveat is that the CTE corrected data are only plotted for stars for which a positive flux is measured in the short exposure. While this is clearly a sensible choice, it excludes some of the faintest objects. However, the bias induced by such a selection is negligible for stars > 50,000e^- in the F606W, since the number of stars with negative flux is negligible in that range (we remind the reader that 50,000e^- in

F606W would imply an average flux of ~50e$^-$ in the short exposure). For fainter stars, the distribution of stellar fluxes is centered at an even lower flux, and the scatter is significantly higher. Therefore the fraction of stars with negative flux increases at low fluxes, and the average values plotted on the Y-axis may be biased towards higher values. However, note that since the average percentage is ~0.1% in all panels, even if the results for the faintest stars were biased, that would imply that the "true" value is <0.1% for those stars. Therefore, that would correspond to a worsening of the CTE with respect to the expected behavior modeled with our CTE correction, which in any case would contradict the hypothesis that CTE is improving at low fluxes.

Summarizing, we confirm that no evidence for significant deviations from the derived CTE model is found at low stellar fluxes.

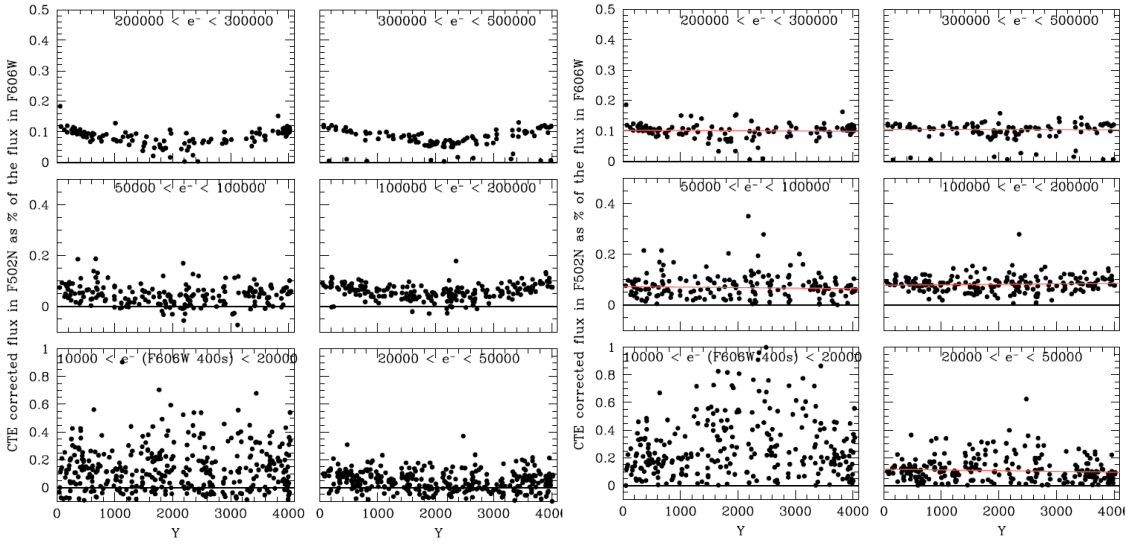

Figure 10: Left: Stellar flux measured in the F502N 30s exposure as a percentage of the flux measured in the deep 400s F606W exposure plotted vs the Y coordinate of each star in the *flt* framework. Left: uncorrected data. Right: data after CTE correction. The red lines are simple linear fits that are just used to guide the eye in identifying the 0.1% expected fraction, in each bin of stellar flux (see text for more details).

Comparison with the pixel-CTE correction

We also compare the CTE correction formula with the results of aperture photometry performed on *DRC* images (i.e. on drizzled images corrected using the pixel-based CTE correction, Anderson & Bedin ISR 2010-03, Anderson & Bedin 2010). To that aim, we again use data from the External CTE monitor calibration program. We use the large slews as explained above to compare the fluxes of stars measured at different distances from the amplifiers. We proceed in the same way as explained in Sect. "Results" and we fit the magnitude residuals across the whole chip in order to derive the average magnitude

loss at Y=2000 transfers. The analysis is performed both on uncorrected data (*DRZ*) and on the *DRC* files. In Fig. 11 we show the results for data taken with F502N 30s exposure time (left) and F606W 400s exposure time (right). The residual magnitude loss at Y=2000 after CTE correction is plotted for different bins of stellar flux measured within the 3 pixel aperture radius. For the non-corrected data, Δmag is the actual magnitude loss. It is clear that while the CTE correction formula and the pixel based CTE correction substantially agree for relatively high background levels, the CTE formula (3) produces significantly more accurate results at low sky levels.

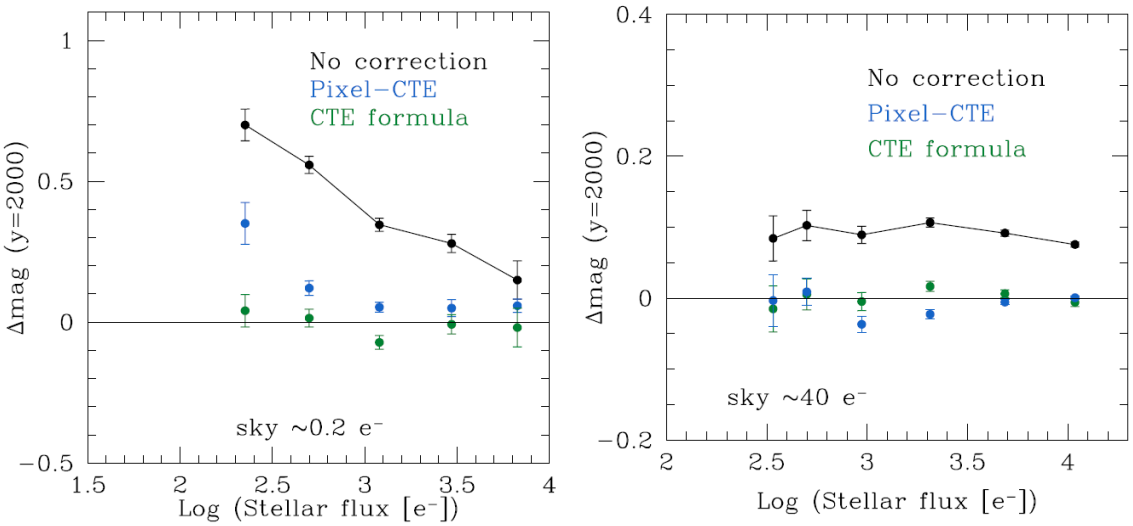

Figure 11: Residual magnitude losses at Y=2000 transfers after CTE correction for stars in different bins of flux. For the non-corrected data the actual magnitude loss is plotted. On the left-hand side data taken with F502N and 30s exposure time are shown. On the right-hand side data taken with F606W and 400s exposure time are shown. Photometry is performed on images taken in Cycle 18.

CTE correction cookbook

In this section we quickly describe the procedure that users should follow in order to correctly apply the CTE correction formula.

1. Obtain *FLT* images using CALACS, and then use *Multidrizzle* or *Astrodrizzle* to obtain *DRZ* data. Alternatively, one can use the *DRZ* files from the pipeline, as provided by the MAST.

2. Multiply the *DRZ* images by the exposure time. *In case multiple exposures are combined in a single final drizzled image, the exposure time of the single exposure should be used. In case the exposures were taken with different exposure times, we recommend that the photometry be performed on each of the images separately. The results can then be corrected for CTE losses and finally averaged*

to obtain a more accurate measurement of the stellar flux.

3. Perform aperture photometry with any preferred software (e.g. *daophot*). Set the photometry aperture radius to r=3 pixels. Measure the background for each star locally (e.g. in an annulus of r_{min}= 13 pix and r_{max}= 18 pixels, centered on the star).

4. Obtain the epoch of the observation in modified Julian days (MJD) from the header keyword EXPSTART (or EXPEND).

5. Measure the number of transfers for each star. The number of transfers are best obtained by identifying the position of each star on the *FLT* image. To that aim, one can either use the task "tran" in PYRAF, or measure the coordinates of the stars directly on the corresponding *FLT* image. For stars that fall in WFC2 (which is included in extension [1] of the *FLT* fits file), the number of transfers Y_{tran} is simply the y coordinate of the star. For WFC1, which is included in extension [4] of the same fits file, the number of transfers is Y_{tran}=2049-y_{star}, where y_{star} is the y coordinate of the star on that frame. *Note that this needs particular care in case the observations are dithered. If the position of the star changes only by a few (< 10) pixels, the correction is still well within the error even for large losses. However, if the dithers imply larger shifts, the user should carefully check the original position of each star in the FLT files, and then derive the correction using the average value of* Y_{tran}. *While doing so, it is also recommended to make sure that the parameters used in multidrizzle (or astrodrizzle) do not generate any biases when the CR rejection is performed.*

6. Apply formula (3) using FLUX = stellar flux measured within the aperture radius (in electrons), SKY = local background for each star (in electrons), t = t(MJD) observation date in modified Julian days.

7. Apply the magnitude correction to the results of the performed photometry (in magnitudes, e.g. $mag_{corrected} = mag_{measured} - \Delta mag$).

8. Perform the aperture correction (see Sirianni et al. 2005).

Any additional correction (i.e. transforming the flux from [e^-] into [$e^- s^{-1}$] and applying the zeropoints to transform the flux into AB or Vega magnitudes) should be performed after all of the above steps.

Users should be reminded that the formula was calibrated using stellar fluxes between ~50 e^- and ~80,000 e^- (measured within the 3pixel aperture radius), and for background levels between ~0.1 and ~50e^-. Therefore, *to ensure the highest level of accuracy, the formula should be used to correct photometry of stars that are within the range specified above*. However, note that for stellar fluxes and background levels higher than the above limits the amount of the correction is <2% even for stars located at the edge of the chip, far from the amplifiers. For very bright stars the CTE formula currently over-estimates CTE losses. For the specific case of very bright stars, the use of *FLC* and *DRC* files (i.e. those obtained with the pixel-based CTE correction included in the ACS pipeline) is a better option.

Conclusions

We derived a new accurate photometric CTE correction formula for point sources. The formula should be used to derive optimal corrections for aperture photometry of ACS/WFC point sources in images taken after SM4 (HST Cycle 17 and later). For data taken in earlier Cycles the formula given in Chiaberge et al. (2009) may still be used without significant loss of accuracy. The new formula is provided for photometry obtained with a 3-pixel aperture radius, but will be extended in the future to different aperture radii. We will keep the coefficients up-to-date every Cycle when new external calibration data are taken. Therefore, we encourage users to check the ACS CTE website for the most recent updates before performing stellar photometry and CTE correction in order to obtain the latest values of the coefficients. Furthermore, the ACS Team is planning to release a CTE correction web tool that will be available to users in the fall of 2012.

Acknowledgements

M.C. thanks R. Avila, J. Anderson, L. Smith, D. Golimowski, and P.L. Lim for useful discussions and invaluable contribution to this work. Thanks to J. Ely and N. Panagia for insightful discussions on statistical analysis and the use of “R”. Thanks also to Josh Sokol and Sara Ogaz for additional testing.

References

Anderson, J., Bedin, L. 2010, PASP, 122, 1035
Anderson, J., Bedin L., 2012 ACS/ISR 10-03

Chambers, J. M. (1992) *Linear models*. Chapter 4 of *Statistical Models in S* eds J. M. Chambers and T. J. Hastie, Wadsworth & Brooks/Cole.
Chiaberge, M. et al. 2009, ACS/ISR 09-01
Huber, P.J. (1981) *Robust Statistics*. Wiley.
Mack, J., et al. 2007 ACS/ISR 07-02
Mutchler & Sirianni 2005, ACS/ISR 05-03
Pickel, J.C., Kalma, A.H., Hopkinson, G.R., and Marshall, C.J. 2003, IEEE Trans. Nucl. Sci. vol 50, 671.
Reiss, A., 2003, ACS/ISR 03-09
Sirianni, M., et al 2005, PASP, 117, 1049
Srour, J.R., Marshall, C.J., and Marshall, P.W. 2003, IEEE Trans. Nucl. Sci. vol 50, 653.
Ubeda, L., Anderson, J., 2012, ACS/ISR 12-03